

IMPULSIVE ACTIONS DUE TO SEISMIC JERK AND DESIGN OF REINFORCEMENTS TO COUNTERACT THEIR EFFECTS IN MASONRY BUILDINGS

Massimo Mariani¹ and Francesco Pugi²

¹ Studio Ricerche Applicate
06123 Perugia, Italy
ricercheapplicate@libero.it

² Aedes Software: Ricerca e Sviluppo
56028 San Miniato, Pisa, Italy
info@aedes.it

Abstract

Studies on the impulsive content of seismic acceleration have highlighted the close correlation between damages caused by jerk and local failures with eventual trigger of chaotic collapses. The impulsive hammering actions can in fact generate stress concentration and consequently disaggregation. This study investigates the potential causes of structural node failures and identifies the interventions able to counteract the effects of jerk, particularly in the case of rubble stone masonry with low-quality mortar. Containment of masonry and placement of tensile-resistant elements designed to absorb the impulsive stresses proved necessary. Placement of additional transversal elements constitutes a natural extension of reinforced plaster interventions, both with traditional and modern techniques such as FRCM. Through additional bent elements, the continuity of the reinforced plaster at the structural connections can be ensured. This aspect is often overlooked particularly in the connections between load-bearing walls and internal floor slabs. The interruption of reinforced plaster at the extrados and intrados of floor slabs constitutes, in fact, an important cause of local vulnerability.

Keywords: existing buildings, masonry structures, seismic motion, seismic jerk, impulsive forces, floor-to-wall connection, strengthening interventions

1 INTRODUCTION

Recent works [1, 2] highlighted the role of seismic jerk, defined as the variation of acceleration and expression of its impulsive content. Seismic events even very distant in time and space, confirm, in addition to the spatial nature of the seismic motion, the great relevance of the impulsive actions.

Seismic records of 2023 Turkey-Syria mainshock (MW 7.8, 06.02.2023) show very high peaks of accelerations and jerk. Station TK.3138, located near the seismic fault, recorded a horizontal PGA of 0.907 g and a vertical PGA of 1.309 g (30% higher than gravity acceleration)¹, with peak ground jerk of 67.91 g/s (horizontal) and 88.42 g/s (vertical)²: these are exceptional values, in particular for the vertical component, which was far beyond the structural damage threshold [3].

Sources: ¹ ESM, *Engineering Strong-Motion Database*; ² elaborations with *Seismic3D software*, developed by Francesco Pugi and tested with Massimo Mariani.

Starting from the scientific works produced on this subject, the study of jerk was deepened by elaborating all the available records of the most important seismic events occurred in Italy from 1976 to 2016, for a total of 447 seismic records. Then, through a statistic approach, the main characteristic parameters of jerk were defined: amplitude, frequency and duration, for the three spatial components.

Later, attention was paid to the effects of jerk on structures. The impulsive content of acceleration plays a fundamental role in the local damages, particularly in existing buildings where quality of masonry, constraints and connections between structural elements may not guarantee the strength required by stress concentrations generated by acceleration variations.

There is a close relationship between damages caused by jerk and local crises with potential trigger of chaotic collapses, typical of structures with insufficient robustness. This phenomenology provides an effective path to interpret the damages caused by recent seismic events on existing masonry buildings: collapses caused by disruptive processes where a fundamental role was played by impulsive hammering actions.

Following these considerations, two fundamental aspects have been highlighted:

- formulation of impulsive actions in terms of forces, which generate instantaneous increases in stress with potential failure due to lack of resistance.
- evaluation of jerk frequencies in relation to fundamental periods of structures: resonance amplifies the dynamic effects.

Based on the considered seismic events, a statistical analysis of jerk frequencies was conducted, finding that in vertical direction the jerk mean period is very close to the fundamental periods of structures [2].

In this work, the attention is focused on floor-to-wall connections. Experience indicates that under dynamic seismic action floors hardly collapse due to insufficient strength or excessive deformation: their collapse is more frequently due to failure in the supporting masonry walls.

The portion of masonry walls at the connection with floors is included in the so-called “rigid zone” geometrically defined by the intersection between piers and spandrels, located at the bottom and at the top of masonry piers. Normally, this part of masonry is not considered in the safety verifications, nevertheless, it is site of local phenomena which can play a fundamental role for equilibrium, particularly in relation to impulsive actions.

The mass associated to the floor-to-wall node is considered affected by an impulsive force due to jerk, which acts in combination with the state of stress due to static and seismic inertial actions. The impulsive action may be entrusted to dedicated resisting elements, in order to define integrative strengthening interventions.

The impulsive effects are particularly important for rubble stone masonry with poor quality mortar. In these cases disaggregation must be prevented and, although the additional strengthening measure are designed according to the expected seismic event, it is always advisable to intervene with the improvement of constraints and masonry quality.

Masonry typologies with higher mechanical characteristics, such as solid bricks with good quality mortars, may absorb the local impulsive effects without the need of additional strengthening elements on top of those eventually required according to common static and seismic verifications. However, beyond the numerical evaluation, at each state of the project particular attention must be paid to connections between structural elements and to discontinuities of various origins. In fact, in these areas of the construction, concentration of stress due to impulsive effects could, in any case, weaken the structural capacity.

Ultimately, a strengthening intervention must ensure the proper connections between floors and load-bearing walls, as well as guarantee the equilibrium of the constraints inserting where necessary integrative tensile resistant elements, aimed at preventing local failures under impulsive effects.

2 OVERVIEW OF JERK FUNDAMENTAL ASPECTS

The chaotic nature of the seismic motion is highlighted by the three-dimensional representation of the accelerograms, that is, the 3D path outlined by the acceleration vector (applied in the origin of the system) with its sharp variation in magnitude and direction.

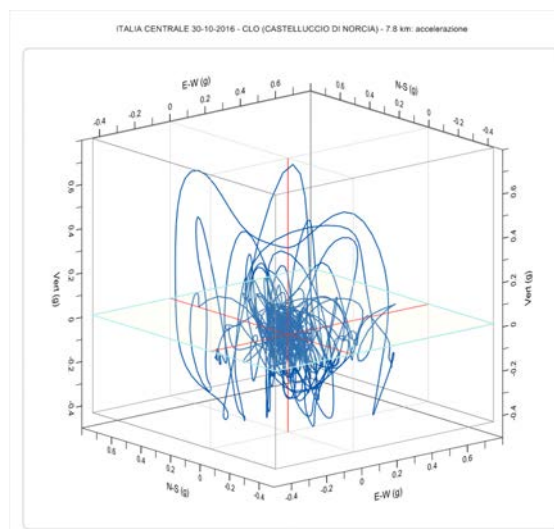


Figure 1. 3D Accelerogram at Castelluccio di Norcia (CLO) during 30.10.2016 Norcia mainshock

The 3D accelerograms indicate a new perspective in the study of the shape of the curves and their evolution throughout the duration of the seismic event. The continuous alterations of the acceleration vector in terms of magnitude and direction suggest to further investigate on the variation of acceleration [1].

The seismic ground acceleration determines structural accelerations which are strictly related to stress and deformation in the resistant elements. From the complexity of the seismic motion the following consideration arises: the safety verification applied in terms of resistance and deformation under inertial forces, may not be enough to fully describe the structural response. The assessment of the structural capacity of the resistant element cannot ignore verifications in terms of impulsive effects, that are the forces appearing in short time intervals in which the state of stress changes: increases, decreases or changes sign.

Studying the variation of acceleration means studying the time derivative of acceleration (TDoA), that is the velocity of acceleration or the third derivative of displacement, referred to as jerk and associated to the symbol j .

In Seismic Engineering, displacement, velocity, and acceleration are the motion parameters always used to characterize the seismic event and its effects on structures. The seismic jerk, that only in recent years has been object of attention, had so far little or no application neither in the design of new structures nor in the assessment of existing buildings and the design of strengthening interventions. Tong et al. (2005) [3] investigated on seismic jerk starting from the need of obtaining quantitative understanding about its amplitude, duration, and frequency content. The study is based on records from the 1999 Chi-Chi Earthquake in Taiwan (M_w 7.6, 17:47, 20.09.1999) and one of its aftershocks (M_w 6.2, 00:14, 22.09.1999). At that time, jerk sensors were not widely available; therefore, jerk time series were obtained from ground acceleration records via numerical methods. Accelerometers provide seismic acceleration as a discrete signal; therefore, seismic jerk can be calculated by the following mid-point differentiation formula:

$$j(t_i) = \frac{a(t_{i+1}) - a(t_{i-1}))}{2\Delta t} \quad (i = 2, \dots, N - 1) \quad (1)$$

where: $a(t_i)$ is the acceleration at instant t_i ; N is the number of samples; Δt is the sampling period. The formula is applied separately for each of the three components of the jerk vector $j = \frac{da}{dt}$.

The variation of jerk can be represented both as time series of its three components and as 3D path outlined by the jerk vector in space (like the ones shown for acceleration). In the 3D path outlined by acceleration vector it is worth noticing that jerk vector is tangent to the path in each point.

In order to understand the relationship between acceleration and jerk let us consider the ground acceleration records at station CLO (Castelluccio di Norcia) during 30.10.2016 Norcia earthquake in Central Italy (mainshock). In particular, let us consider the vertical acceleration time series focusing on a small time interval between 19.3 s and 19.8 s (0.5 s) in which both PGA and PGJ occur.

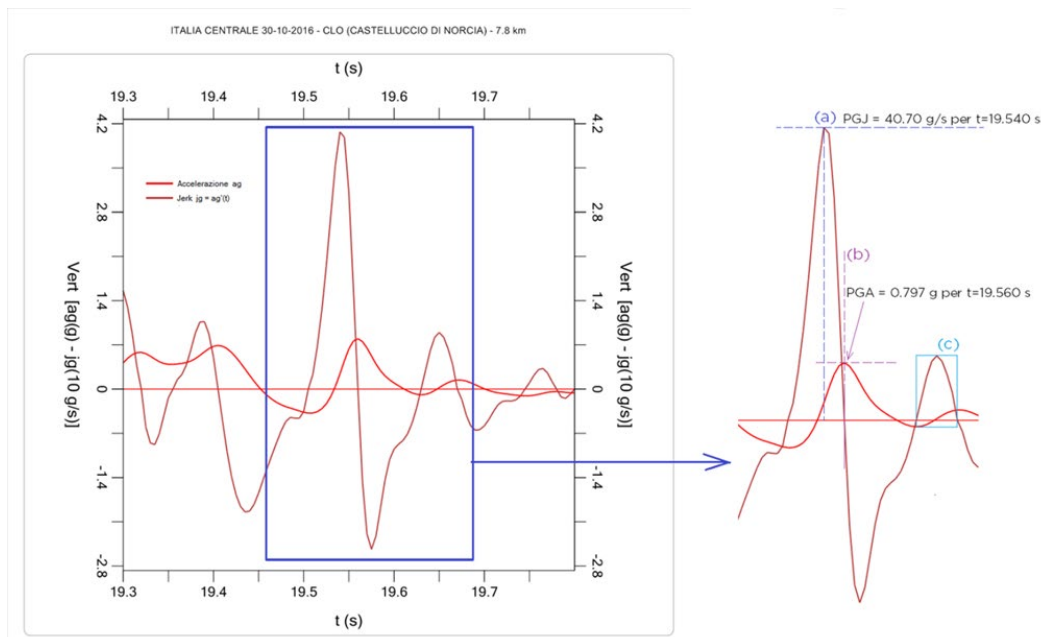


Figure 2. Comparison between acceleration and jerk time series. The detail on the right shows how the points where jerk is zero correspond to local maximum or minimum of acceleration.

Since jerk is the first derivative of acceleration it is equal to zero when acceleration shows a local maximum or minimum.

The detail in Figure 2 highlights (a) the absolute maximum of jerk (PGJ); (b) the absolute maximum of acceleration correspondent (like other local maximum) to zero in jerk; (c) the sector between two consecutive zeros of jerk correspondent to local minimum and maximum of acceleration.

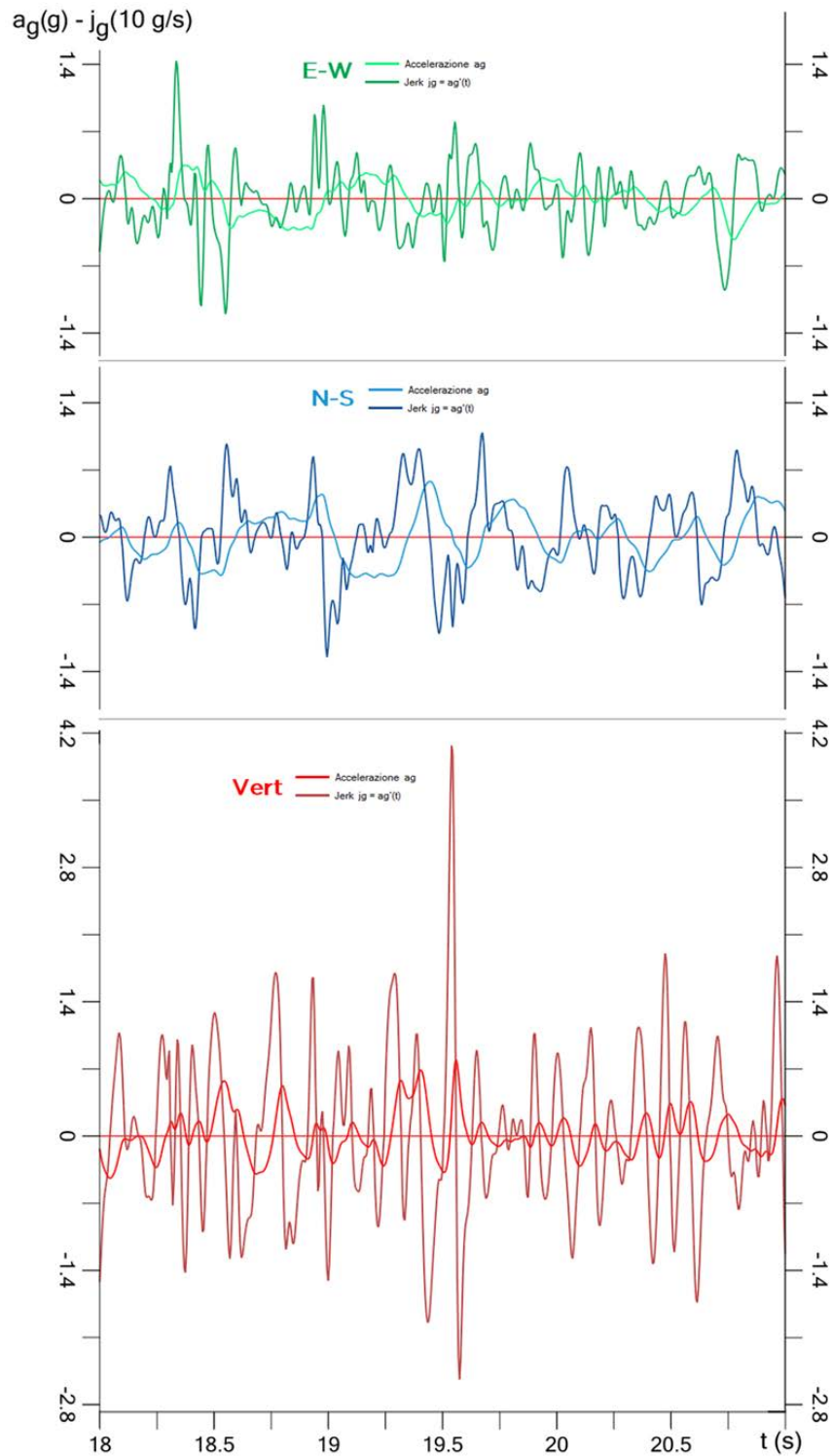


Figure 3. Acceleration and jerk time series for the three components (EW, NS, Vert)

Figure 3 shows the time series of acceleration and jerk for the three components in the time span between 18.0 s and 21.0 s . Jerk time series feature a higher number of fluctuations between positive and negative values: this is even more evident from the detail in Figure 4. Throughout the seismic event, the secondary fluctuation of acceleration corresponds to significant jerk peaks of alternate sign. The operation of derivation generates a “jerk” function characterized by denser peaks, that is, in strict terms, by higher frequencies.

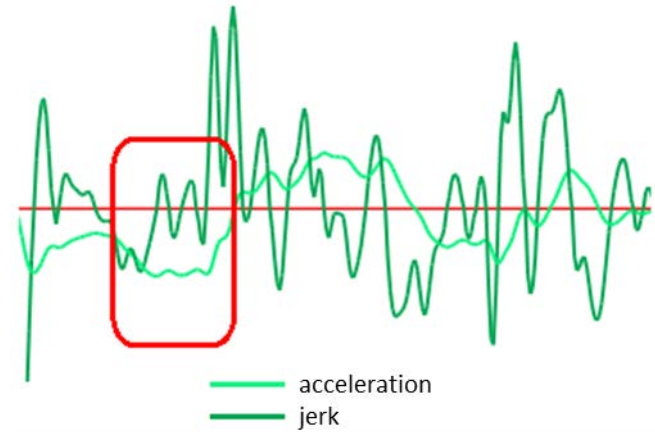


Figure 4. Secondary fluctuation of acceleration correspondent to jerk peaks

The 3D paths outlined by the jerk vector are similar to those already seen for acceleration. Comparison between acceleration and jerk paths is given in Figure 5.

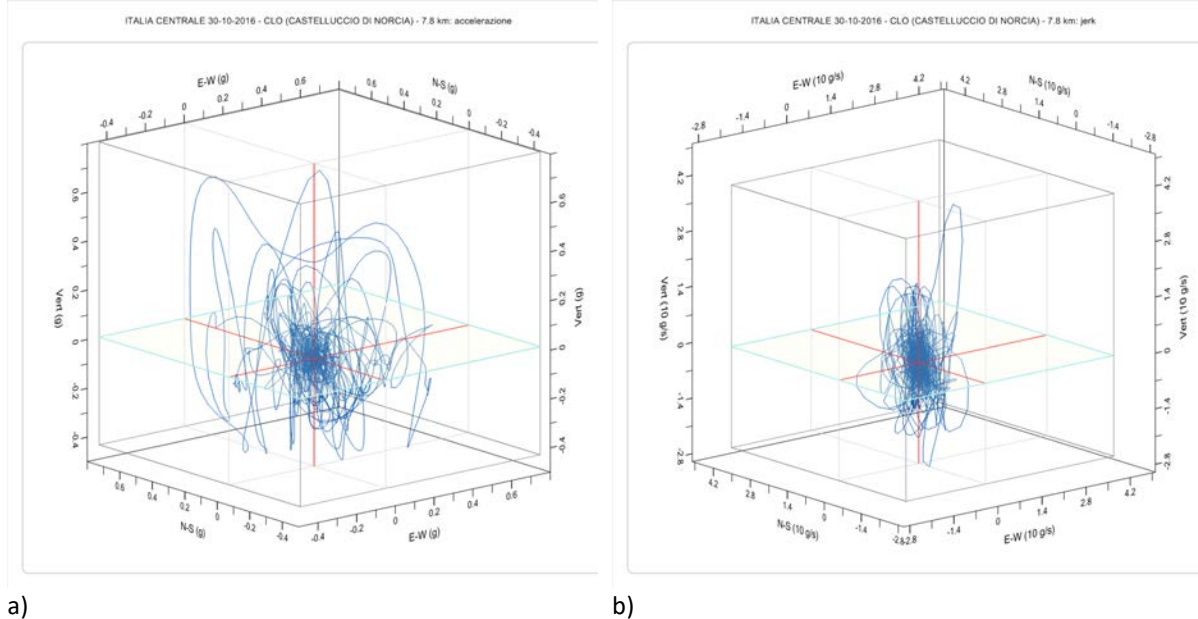


Figure 5. Comparison between (a) acceleration and (b) jerk paths: 3D view

Figure 6 shows the comparison between acceleration and jerk 3D paths projected on a vertical plane. The jerk tangle appears stretched in the vertical direction and this points out the importance of the vertical seismic component [4, 5].

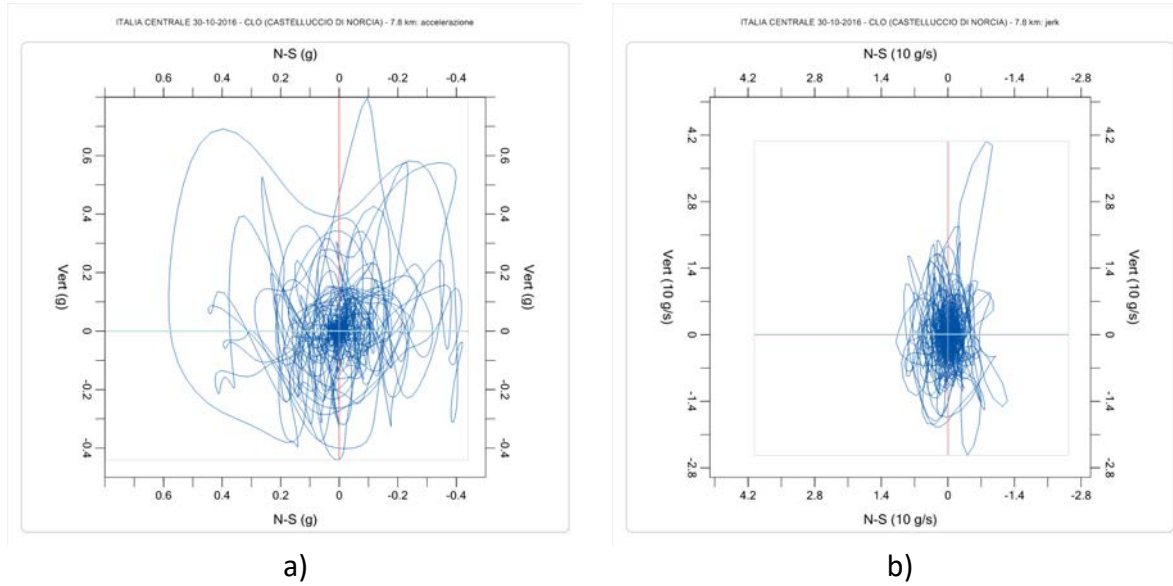


Figure 6. Comparison between (a) acceleration and (b) jerk paths: projection on vertical plane NS-Vert

During a seismic event, ground acceleration varies quickly, and the correspondent inertial forces also fluctuate in short time intervals of the order of few milliseconds. This sharp variation causes “jolts”, that is, impulsive forces that act very briefly. Therefore, for jerk to become a useful parameter in structural analysis, it should be considered along with the corresponding impulsive forces. A new approach is introduced below.

Impulsive forces due to seismic jerk are distinct from inertial forces due to acceleration. The former are generated by the variation of acceleration and may be much higher than the latter. Their influence on a structure depends on the frequency content of the jerk and the dynamic properties of the structure itself.

The integral of jerk is, by its own definition, an acceleration. Since acceleration, according to Newton’s Second Law, is force per unit mass, the definite integral of jerk in the interval between two consecutive zeros may be referred to as “impulsive force per unit mass” (F_{imp}/m). Two consecutive zeros of jerk correspond to a maximum and a minimum of acceleration, or vice-versa. The signed area bounded by the jerk function in that interval corresponds to the impulse of acceleration or deceleration. Therefore, considering the interval between instants t_1 and t_2 , the impulsive force per unit mass is given by:

$$\frac{F_{imp}}{m} = \int_{t_1}^{t_2} j(t) dt \quad (2)$$

This expression can be applied to any of the three jerk components, each one characterized by its own sequence of zeros.

Figure 7 illustrates the definition of impulsive force per unit mass as the area bounded by the jerk function $j(t)$ between two consecutive zeros. Yellow color indicates the positive impulsive force corresponding to an interval where acceleration increases: $a(t)$ goes from a minimum to a maximum. Instead, green color indicates a negative impulsive force corresponding to the interval where acceleration decreases going from a maximum to a minimum. Therefore, the impulsive force in the interval (t_0, t_1) and the one in the interval (t_1, t_2) act in opposite direction.

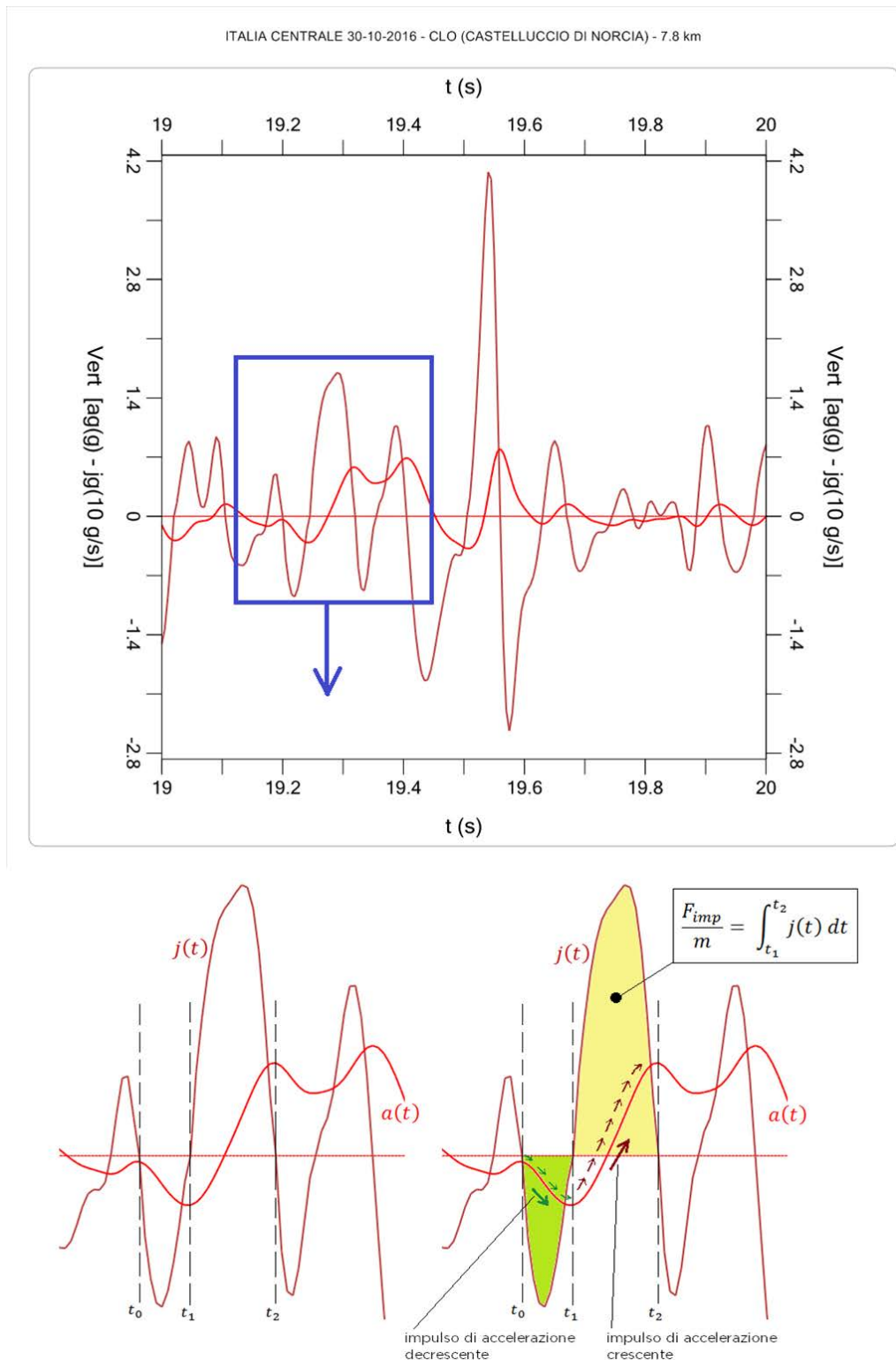


Figure 7. Impulsive force per unit mass, defined as the integral of jerk between two consecutive zeros.

Figure 7 refers to the vertical component of the ground motion recorded at station CLO (Castelluccio di Norcia) during 30.10.2016 Norcia mainshock in the time interval (19.000 – 20.000 s).

It is worth noticing the very short duration of the impulsive forces. The considered jerk zeros correspond to the following instants in the record: $t_0 = 19.200$ s, $t_1 = 19.245$ s, $t_2 = 19.320$ s.

The negative impulsive force corresponding to decreasing acceleration lasts 45 ms while the following positive impulsive force lasts 75 ms.

Thus, impulsive force may be calculated throughout the record for each time interval between two consecutive jerk zeros. The result is a step function that represents the time series of impulsive force per unit mass.

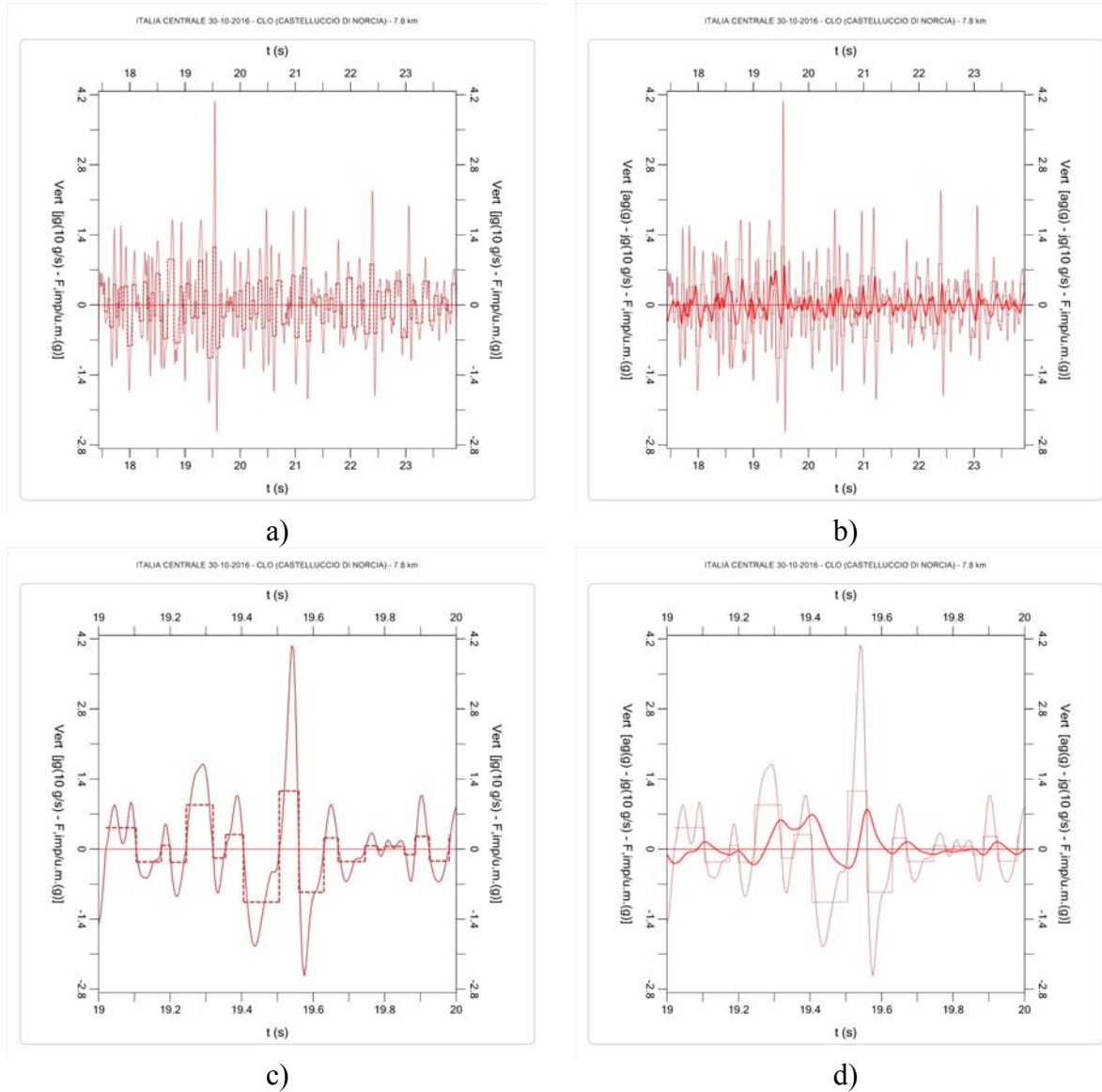


Figure 8. Jerk and impulsive forces per unit mass for the vertical seismic component.
CLO – 30.10.2016 Norcia mainshock

Figure 8 shows the jerk time series (solid line) and the step function of impulsive forces per unit mass (dashed line) for the vertical component of the reference seismic motion. The graphs on the right (b, d) also display the correspondent acceleration time series. The graphs at the top (a, b) refer to the time span between first and last acceleration peak exceeding 0.250 g, while the graphs at the bottom (c, d) refer to a shorter time interval (19.000 – 20.000 s).

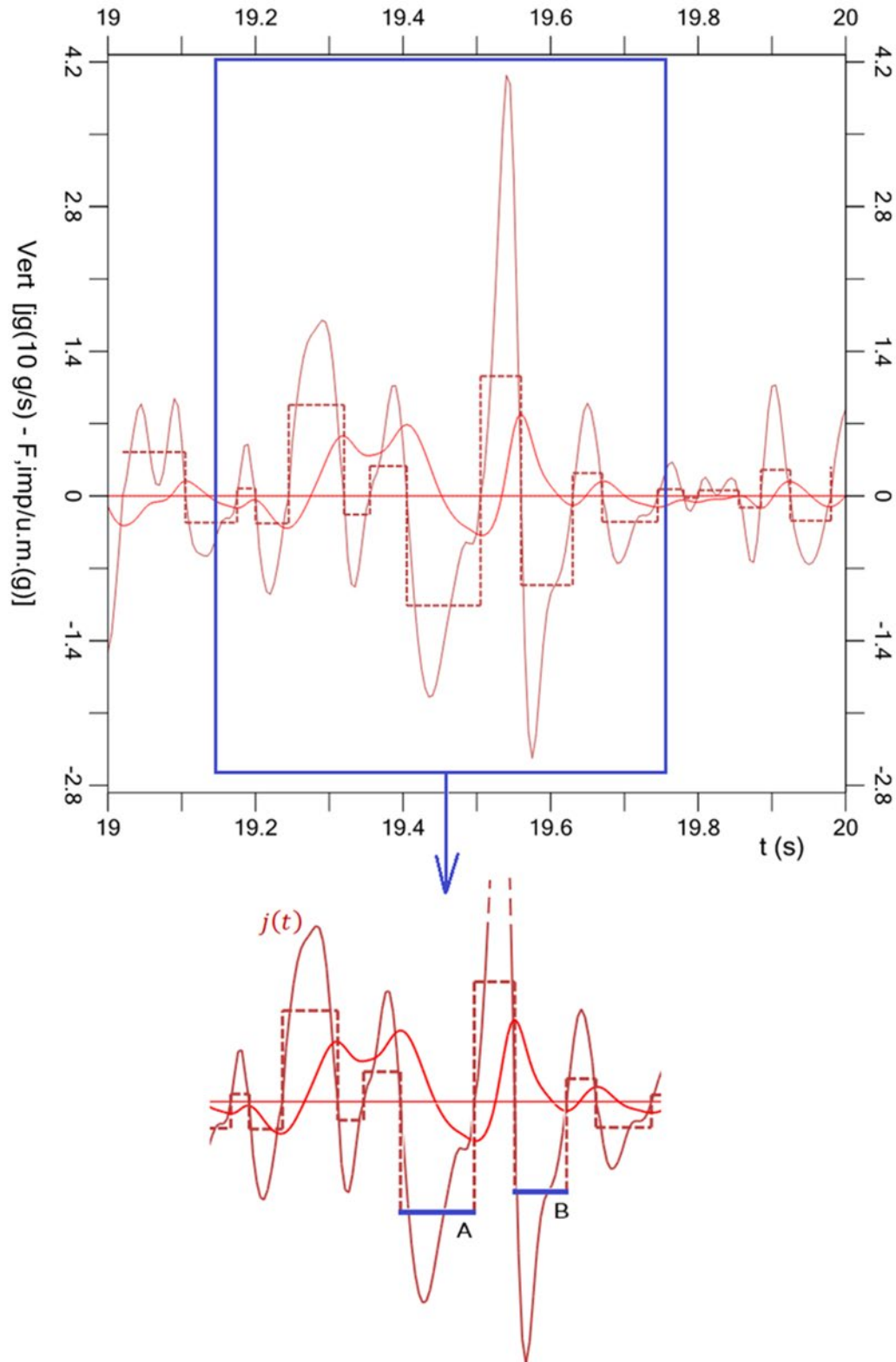


Figure 9. Peaks of jerk and correspondent impulsive forces

The detail shown in Figure 9 highlights an important aspect: the peak of jerk does not always correspond to the peak of impulsive force. This is because the impulsive force does not depend

only on the jerk value but also on the length of the time interval between two consecutive zeros. Therefore, lower jerk peaks with longer duration may yield higher impulsive forces than higher jerk peaks with shorter duration (cf. Impulsive forces A and B in Figure 9).

This behavior has general validity, it applies to all the components of seismic motion and different seismic events: the maximum values of jerk and impulsive force do not occur at the same time. The same happens between peaks of acceleration and peaks of jerk. Therefore, we get to the following property: PGA , PGJ and $F_{imp,max}$ are not simultaneous and there is not a direct relationship between them. However, a correlation may be pursued from a statistical perspective.

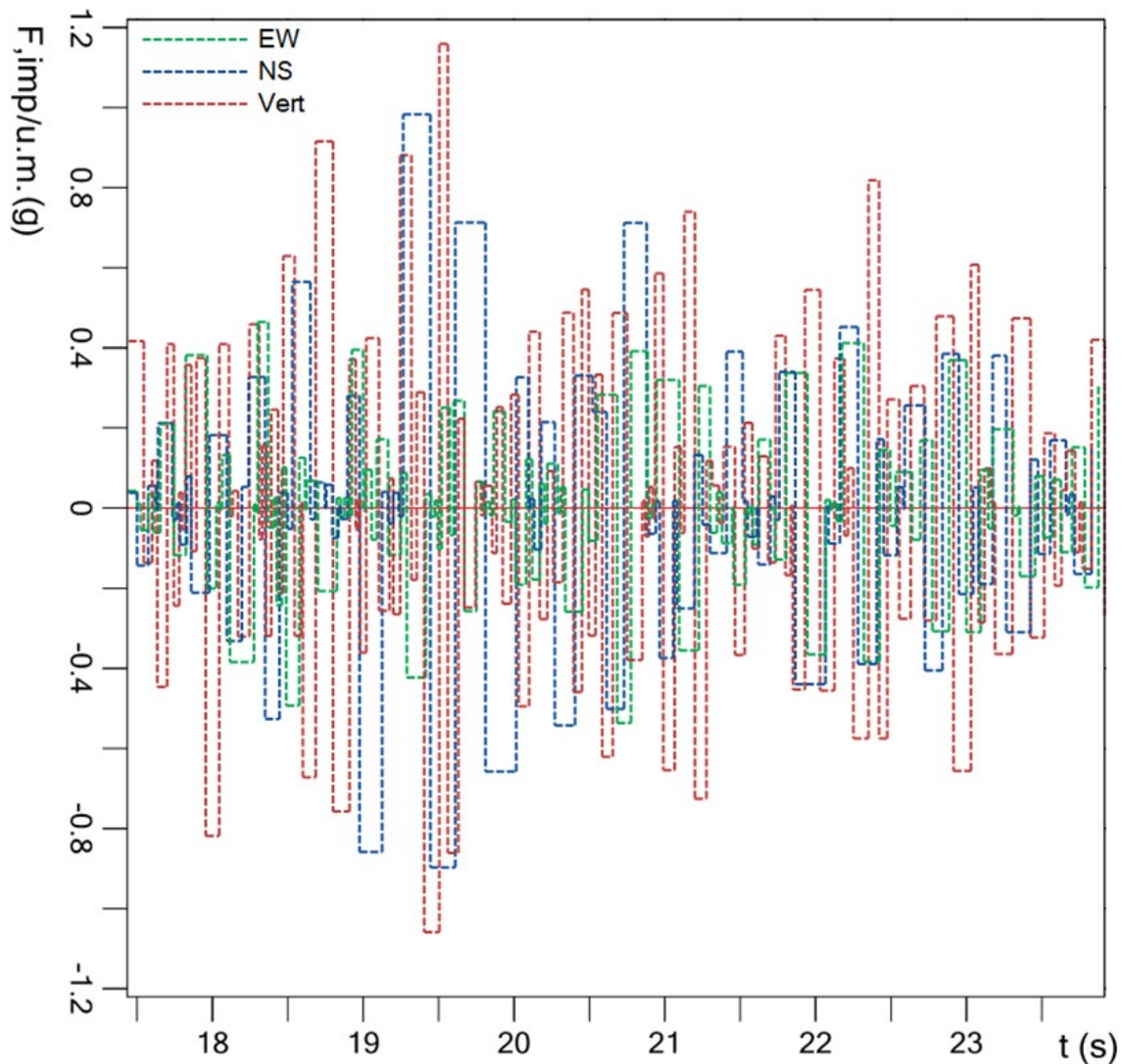


Figure 10. Time series of impulsive force per unit mass. Three components overlaid.

Figure 10 shows the time series of the three components of impulsive forces overlaid in the same graph.

Thus, considering jerk, the dynamic nature of the seismic action is expressed by a series of consecutive impulses which determine vibrations.

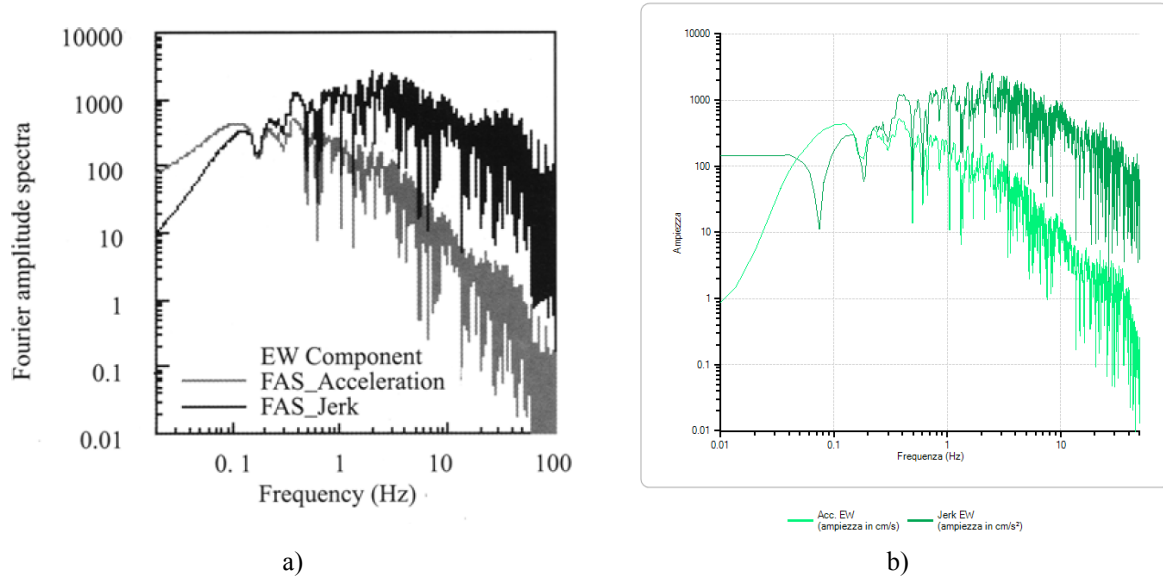


Figure 11. Acceleration and Jerk Fourier amplitude spectra (Chi-Chi 20.9.1999, TCU068, EW component): (a) Tong et al. [3]; (b) Mariani and Pugi [1]

Tong et al. (2005) [3], in their study on the 1999 Chi-Chi earthquake in Taiwan, provided Fourier amplitude spectra both for acceleration and jerk (Figure 11). The dominant frequency contents of acceleration and jerk time series are between 1 and 10 Hz; however, jerk distributes in a much wider frequency band and its higher frequency contents are prominent: the region of significant frequencies for jerk extends at least up to 30 Hz.

This characteristic, observed for the first time in this seismic event in Taiwan, is confirmed for all seismic events in the Italian territory [1]: the jerk Fourier spectrum features a window of dominant frequency wider than the acceleration one. The jerk higher frequency content appears more important.

The identification of the dominant frequency of the seismic motion is crucial for the comparison with the natural frequencies of structures. According to Rathje et al. [14] the parameter that better characterizes the frequency content is the mean period T_m , defined as the average of periods in the Fourier spectrum, each weighted by the square of its Fourier amplitude.

$$T_m = \frac{\sum_i c_i^2 \cdot \left(\frac{1}{f_i}\right)}{\sum_i c_i^2} \quad \text{with } 0.25 \text{ Hz} \leq f_i \leq 20 \text{ Hz} \quad (3)$$

A first example of Fourier analysis with determination of the mean period has been performed on the seismic records from station CLO (Castelluccio di Norcia) during 30.10.2016 Norcia earthquake. Table 1 gives the mean period of acceleration and jerk for the three components of the seismic motion (EW, NS, Vert), while Figure 12 shows the Fourier amplitude spectra of acceleration and jerk for the vertical component.

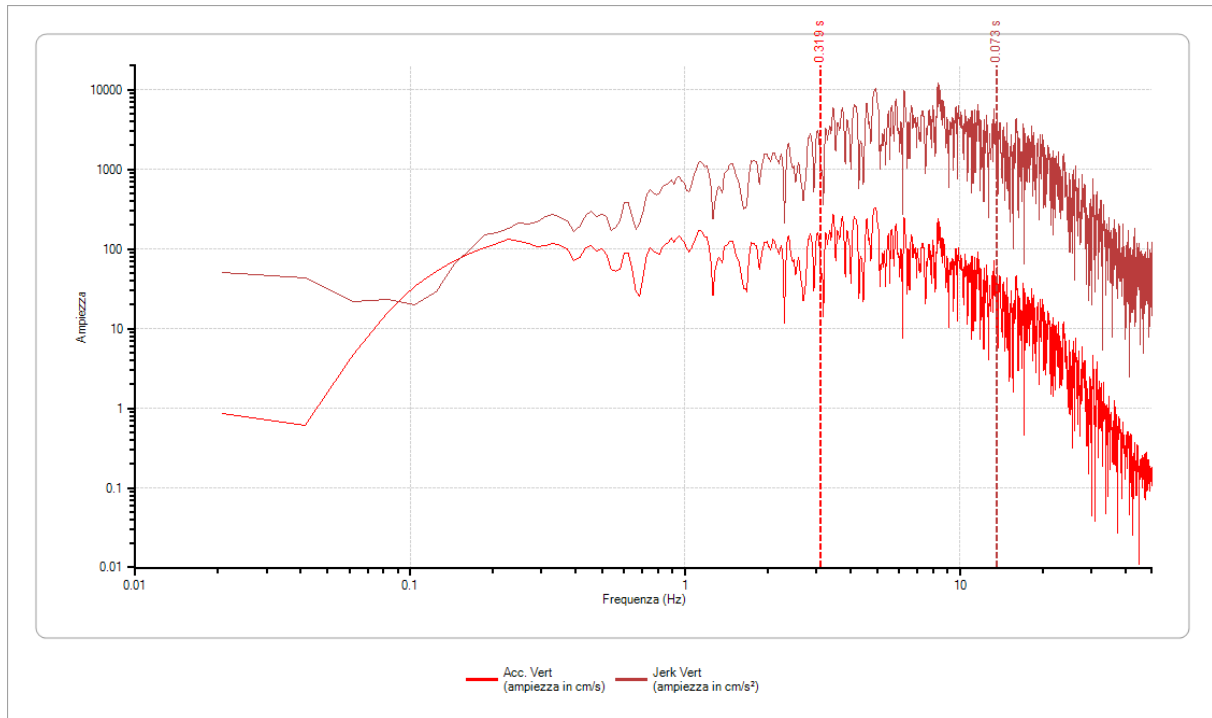


Figure 12. CLO, 2016 Norcia earthquake:
acceleration and jerk Fourier amplitude spectra for vertical component

| $T_m(s)$ | EW | NS | Vert. |
|--------------|-------|-------|-------|
| Acceleration | 0.657 | 0.540 | 0.319 |
| Jerk | 0.107 | 0.137 | 0.073 |

Table 1. Mean period of acceleration and jerk. CLO, 2016 Norcia earthquake

Table 1 highlights an important aspect: the impulsive nature of the vertical component. The main frequencies of the vertical component are significantly higher than the horizontal ones. It is also evident that jerk mean periods are very close to common fundamental periods of rigid structures like masonry buildings. This points out the potential issues caused by impulsive action on structural elements.

Given the chaotic nature of the seismic phenomena, to find a correlation between PGA, PGJ and the maximum Impulsive force a statistical elaboration of the seismic records was carried out.

Eight of the most recent seismic events in the Italian territory were considered: 30.10.2016 Norcia; 24.08.2016 Accumuli; 29.05.2012 Emilia; 06.04.2009 L'Aquila; 26.09.1997 Umbria-Marche; 23.11.1980 Irpinia; 19.09.1979 Valnerina; 06.05.1976 Friuli. For each of these events numerous seismic records provided by ITACA (Italian ACcelerometric Archive) were analyzed, for a total of 447 station records.

3 CORRELATION BETWEEN JERK CHARACTERISTICS AND STRUCTURAL DESIGN PARAMETERS

For each analyzed record the following parameters have been calculated:

1. peak ground acceleration (*PGA*)
2. peak ground jerk (*PGJ*)

3. maximum value of impulsive force per unit mass (F_{imp})
4. mean period (T_m) of acceleration and jerk, calculated through Fourier spectra

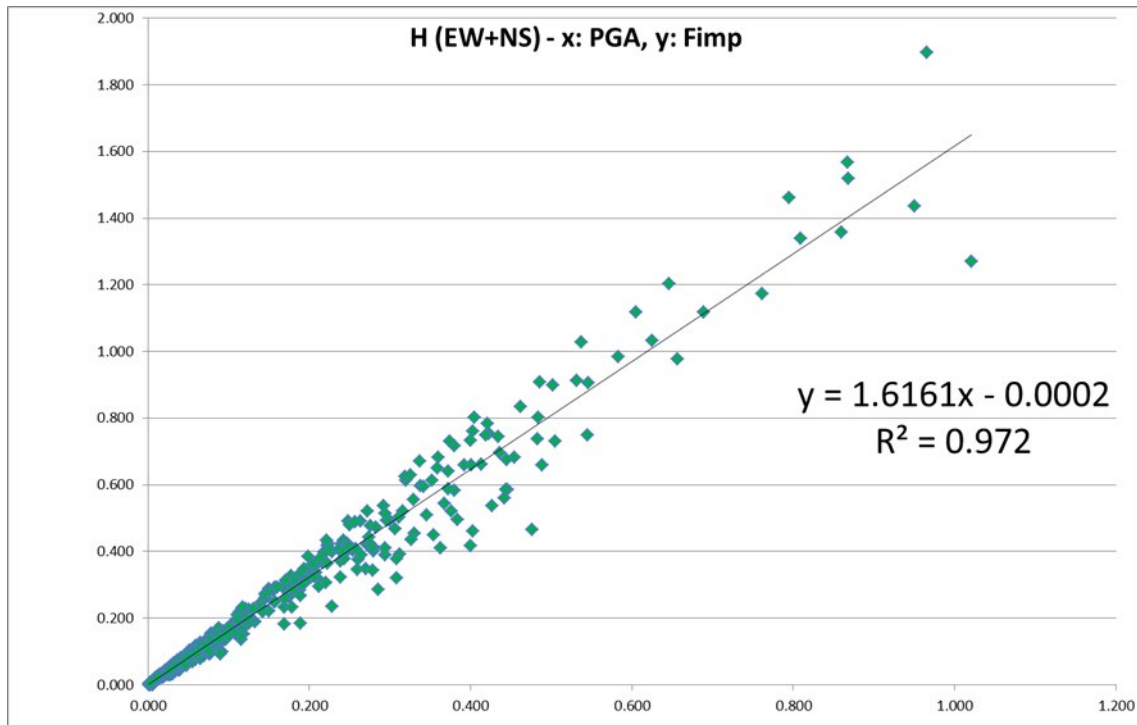


Figure 13. Correlation $PGA-F_{imp}$ for horizontal components

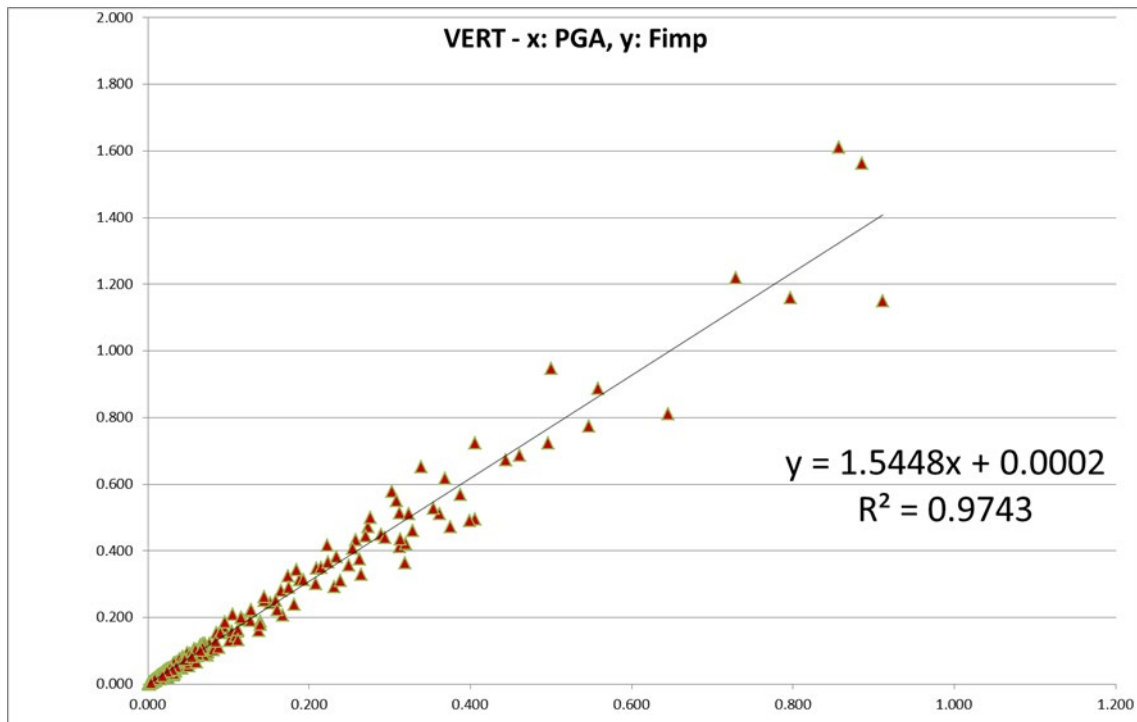


Figure 14. Correlation $PGA-F_{imp}$ for vertical component

Figures 13-14 show the correlation between PGA and maximum impulsive force for unit of mass F_{imp} for horizontal and vertical components.

The correlation between PGA and impulsive forces, obtained through elaboration of the main seismic events in Italy, is an intrinsic property of the events themselves. The fact that the correlation has a coefficient of determination very close to 1 represents an excellent support for estimating the impulsive actions based on ground acceleration data.

The correlation obtained through statistical analysis between PGA and maximum impulsive force per unit mass $F_{imp,max}$, (both expressed in g) are summed up in the following expressions (where: H stand for horizontal component, V stands for vertical component):

$$F_{imp,max,H} = 1.616 PGA_H \quad (4)$$

$$F_{imp,max,V} = 1.545 PGA_V \quad (5)$$

Regarding the frequency analysis, the mean period T_m calculated from Fourier spectra has no relations with peak ground acceleration, peak ground jerk or maximum impulsive forces. In fact, in the single harmonic waves that constitute the signal, amplitude and frequency are mutually independent.

Investigating on the mean periods by direct comparison of the T_m obtained from the 447 station records, a representative value was found in the median value, which compared to the mean value is not skewed by a small proportion of extremely large or small values, and therefore provides a better representation of the center.

Figure 15 shows for the vertical component of jerk the following information:

- a graph showing the mean period T_m for each station considered. The graphs also include the mean value (black line) and the median value (red line) which in all the cases is lower than the mean.
- the frequency distribution with discretization of the periods in intervals of $0.025 s$

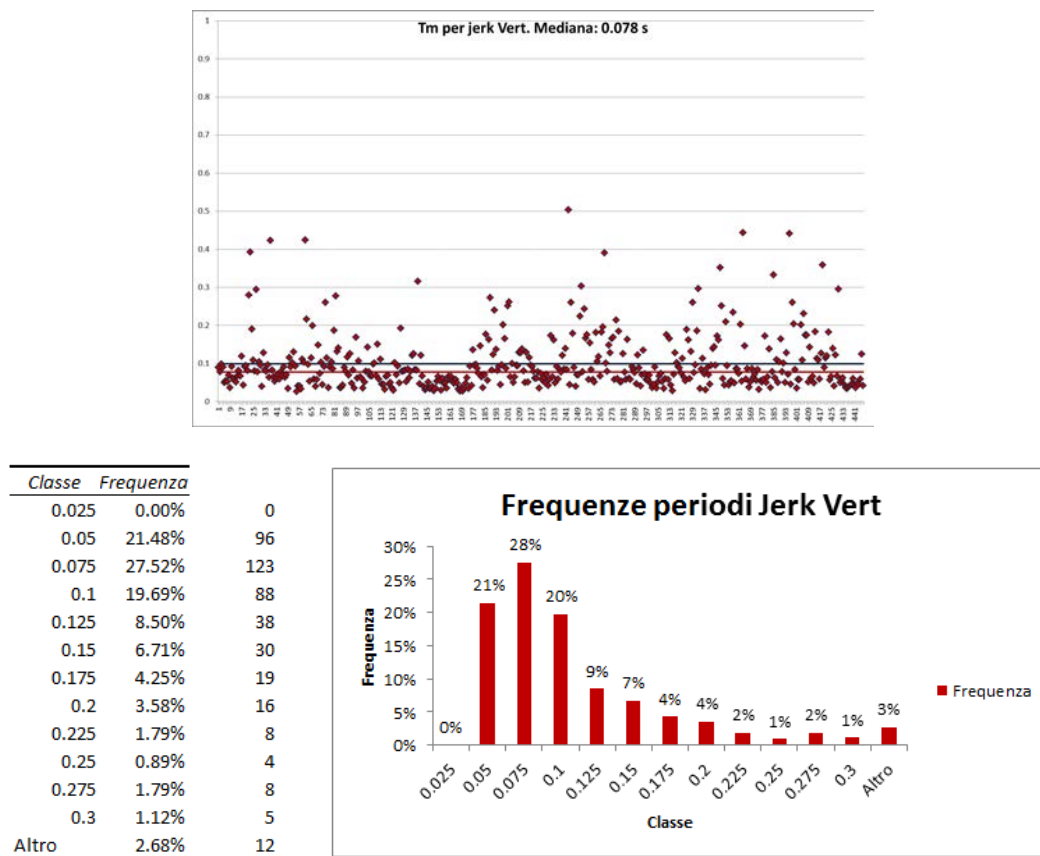


Figure 15. Statistical elaboration on the mean period T_m of vertical jerk

Table 2 sums up the representative values of the mean periods and the main contribution to the distribution, both for acceleration and jerk, for each of the three components:

| Component | $T_m(s)$ and main contribution to the distribution | | | |
|-----------|--|-----------------|-------|-----------------|
| | Acceleration | | Jerk | |
| EW | 0.508 | (19% for 0.500) | 0.102 | (23% for 0.100) |
| NS | 0.509 | (19% for 0.500) | 0.101 | (22% for 0.100) |
| Vert. | 0.506 | (15% for 0.300) | 0.078 | (28% for 0.075) |

Table 2. Representative T_m for acceleration and jerk

The frequency content of vertical jerk is characterized by very high frequencies. The representative value of the mean period T_m is about 0.075 s, which is very close to the vertical fundamental period of many structures characterized by high vertical stiffness. Among them, existing masonry buildings shall be given special attention as they often feature weak connections which may be extremely vulnerable under the effects of impulsive forces.

It is important to notice that other structural typologies may also show local vulnerabilities under impulsive actions. International studies (see references in [1]) take into consideration micro-scale damage of structures where discontinuities are represented by the connections between different structural elements, as in reinforced concrete or steel joints, and not by the constitutive heterogeneity of the material (like in masonry).

To be more specific about the amplification of the structural response in terms of displacements and internal actions, considering that seismic input is a combination of many harmonic excitations, we can refer to the theory of driven harmonic oscillators with viscous damping.

Study of the simple oscillator leads to an amplification factor C_{ampl} given by the following expression:

$$C_{ampl} = \frac{1}{\sqrt{\left(1 - \frac{T^2}{T_1^2}\right)^2 + 4\xi_{eq}^2 \frac{T^2}{T_1^2}}} \quad (6)$$

where: T_1 is the fundamental period of the structure; T is the period of the applied force (in this case coincident with the mean period of vertical jerk component); ξ_{eq} is the equivalent viscous damping coefficient.

The frequency distribution given in Figure 15, obtained from the statistical elaboration of the 447 examined seismic records, clearly shows a log-normal trend.

The jerk mean period of the seismic event that is expected to strike the building is not known and does not depend on the values of PGA and PGJ . Table 3 shows an extract from the list of the 447 examined records with the correspondent value of PGA (g) and jerk T_m (s) with respect to the vertical component, ordered by the value of T_m . For instance, a value of T_m equal to 0.034 s was correspond to many different values of PGA , ranging from 0.071 g to 0.645 g: there is no correlation between T_m and PGA and there are no known studies which identify a possible design value of jerk mean period in a determined site.

Therefore, in the context of design, while PGA assumes precise values given the site of the structure, the same cannot be said for the jerk period. However, it is possible to correlate the jerk mean period to the fundamental periods of the structure using the frequency distribution from a probabilistic perspective.

| Evento-Stazione | PGA VERT | T _m jerk Vert | |
|-------------------|----------|--------------------------|---|
| 06042009_IT_AQA | 0.444 | 0.026 | |
| 29052012_TV_MIR04 | 0.263 | 0.028 | |
| 29052012_TV_MIR02 | 0.461 | 0.028 | |
| 29052012_IV_T0813 | 0.175 | 0.029 | |
| 30102016_IT_ACT | 0.254 | 0.029 | |
| 29052012_IT_SMS0 | 0.104 | 0.03 | |
| 29052012_IV_T0818 | 0.209 | 0.03 | |
| 29052012_IV_T0800 | 0.320 | 0.031 | |
| 30102016_IT_CNE | 0.547 | 0.031 | |
| 30102016_IT_NCR | 0.057 | 0.032 | |
| 29052012_IT_MRN | 0.857 | 0.032 | |
| 29052012_TV_MIR01 | 0.369 | 0.033 | |
| 06042009_IT_AQV | 0.496 | 0.033 | |
| 29052012_IV_T0805 | 0.071 | 0.034 | EMILIA SECOND SHOCK 29-05-2012 - IV_T0805 - 22.0 km - Lat. 44.9187° - Long. 11.3226° - Elev. 5 m |
| 30102016_3A_M263 | 0.112 | 0.034 | ITALIA CENTRALE 30-10-2016 - 3A_M263 - 28.4 km - Lat. 42.62981° - Long. 13.32345° - Elev. 1071 m |
| 30102016_IT_CIT | 0.138 | 0.034 | ITALIA CENTRALE 30-10-2016 - IT_CIT - 26.8 km - Lat. 42.5942° - Long. 13.1632° - Elev. 873 m |
| 29052012_TV_MIR05 | 0.152 | 0.034 | EMILIA SECOND SHOCK 29-05-2012 - TV_MIR05 - 15.8 km - Lat. 44.9808° - Long. 11.10719° - Elev. 0 m |
| 29052012_TV_MIR08 | 0.313 | 0.034 | EMILIA SECOND SHOCK 29-05-2012 - TV_MIR08 - 8.6 km - Lat. 44.9169° - Long. 11.0895° - Elev. 0 m |
| 26091997_IT_NCR | 0.406 | 0.034 | UMBRIA/MARCHE 26-09-1997 - IT_NCR - 10.9 km - Lat. 43.11158° - Long. 12.78467° - Elev. 492 m |
| 30102016_IV_T1214 | 0.645 | 0.034 | ITALIA CENTRALE 30-10-2016 - IV_T1214 - 11.4 km - Lat. 42.75954° - Long. 13.2087° - Elev. 1490 m |

Table 3. Lack of correlation between PGA and T_m

Given the fundamental period of the structure, expression (6) provides the range of jerk mean periods corresponding to a significant amplification factor (e.g. $C_{ampl} \geq 2$). Then, the frequency distribution allows to calculate the correspondent probability of occurrence. This quantitative information constitutes an index of vulnerability of the structure with respect to impulsive actions. In this respect, strengthening interventions determining a reduction of this probability will increase robustness of the structure, that is, its capacity to avoid local damages caused by stress concentration due to jerk.

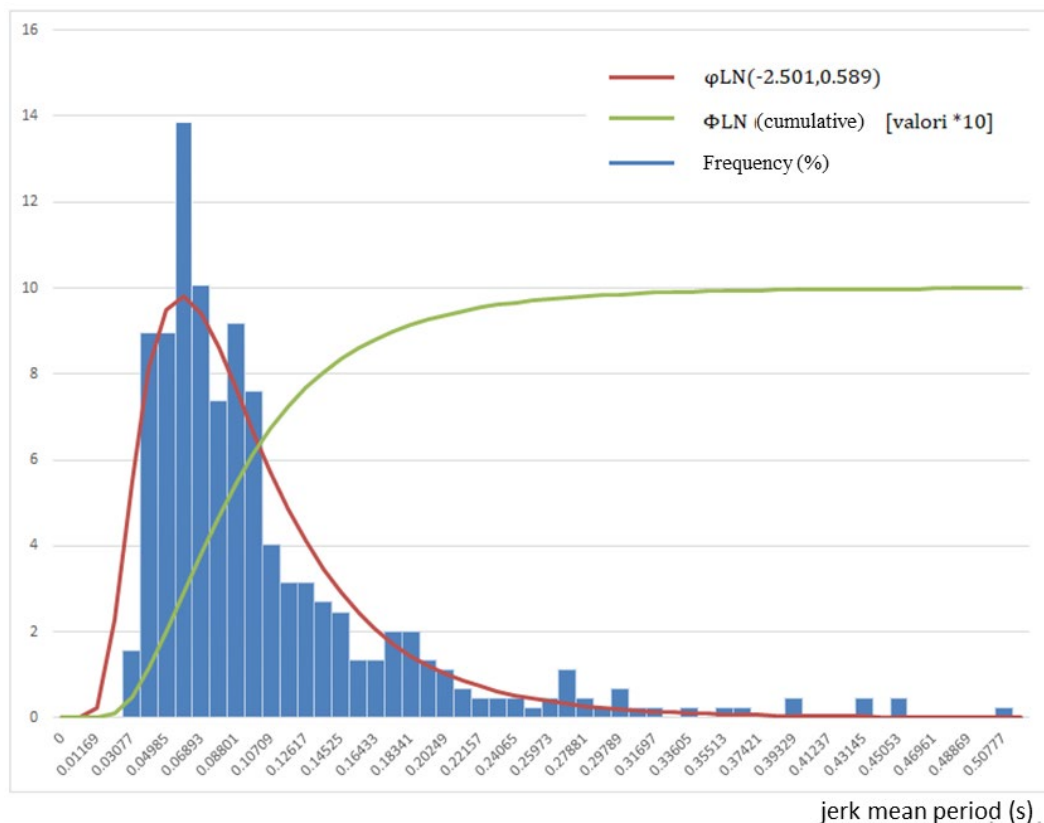


Figure 16. Frequency distribution of vertical jerk mean period

In the graph shown in Figure 16 the X-axis represents the vertical jerk mean period. The histogram represents the frequency distribution calculated for the 447 examined seismic records. The red line is the correspondent log-normal probability distribution of vertical jerk mean period (ϕLN). For a structure with given vertical natural period T_1 , through expression (6) we can identify the interval of jerk mean periods ($T_{jerk,min}, T_{jerk,max}$) for which $C_{ampl} > 1$. These are the jerk frequencies that produce resonance, thus significant amplification of the structural impulsive forces. The green line in the graph is the cumulative probability distribution (ΦLN). The probability that a structure with natural period T_1 enters in resonance with jerk is given by:

$$\Phi LN(T_{jerk,max}) - \Phi LN(T_{jerk,min})$$

For example, let us consider a building characterized by $T_1 = 0.058$ s and $\xi_{eq} = 5\%$. Through expression (6) we find that the jerk mean periods corresponding to $C_{ampl} \geq 2$ are those in the interval (0.048 s, 0.082 s). Using the cumulative probability distribution, we find that the probability of significant amplification of the impulsive actions is:

$$\Phi LN(0.082) - \Phi LN(0.048) = 0.319 = 32\%$$

If the seismic jerk striking this building had mean period equal to the building natural period (0.058 s), the amplification factor would be $C_{ampl} = 10$. Assuming instead $\xi_{eq} = 10\%$ the amplification factor would be $C_{ampl} = 5$: the higher the viscous damping the lower the amplification effect, although it is still quite significant. These considerations will be resumed in the example given in the next section.

Another application of expression (6) is the following. Given a seismic event with known jerk mean period, we can find the interval of building natural periods corresponding to significant amplification of the impulsive actions.

For example, let us consider the aforementioned seismic event 30.10.2016 Norcia, CLO. The calculated jerk mean period is $T = 0.073$ s. Considering $\xi_{eq} = 5\%$, from expression (6) we find that the natural periods corresponding to $C_{ampl} \geq 2$ are those in the interval (0.053 s, 0.113 s). Since the natural period of buildings often falls in this interval, it is reasonable to assume that a substantial number of buildings was affected by amplified impulsive actions.

4 IMPULSIVE ACTIONS IN STRUCTURAL JOINTS: DESIGN OF LOCAL STRENGTHENING MEASURES

The previous section described the characteristics of jerk with particular attention to corresponding impulsive forces and frequency (mean period).

International studies conducted on jerk [2, 3, 7, 8] show that vibrational wave propagation is directly related to stress concentrations and local damages. In this work, particular attention is given to existing masonry buildings where internal connections are often not totally effective: it is, therefore, necessary to investigate on the relation between impulsive actions and local damages, such as masonry disaggregation and connections failure.

Strengthening interventions that confine masonry and absorb local stress concentration improve the structural response to jerk. Considering the very brief duration of impulsive action and the rigid-brittle behavior of masonry, such interventions may be designed in terms of strength.

Let us consider a floor undergoing a conservative intervention as one of the strengthening measures designed for the building. The strengthening is achieved through a lightweight concrete slab built on top of the floor, collaborating with it through a system of connectors. At the constraints, steel bars properly anchored through masonry ensure the connection between floor and perimetral walls (see Figure 17). The usual safety verifications carried out for the floor in

terms of strength and deformability under vertical design actions (permanent, variable, and seismic loading) provide quantification of the improvement achieved.

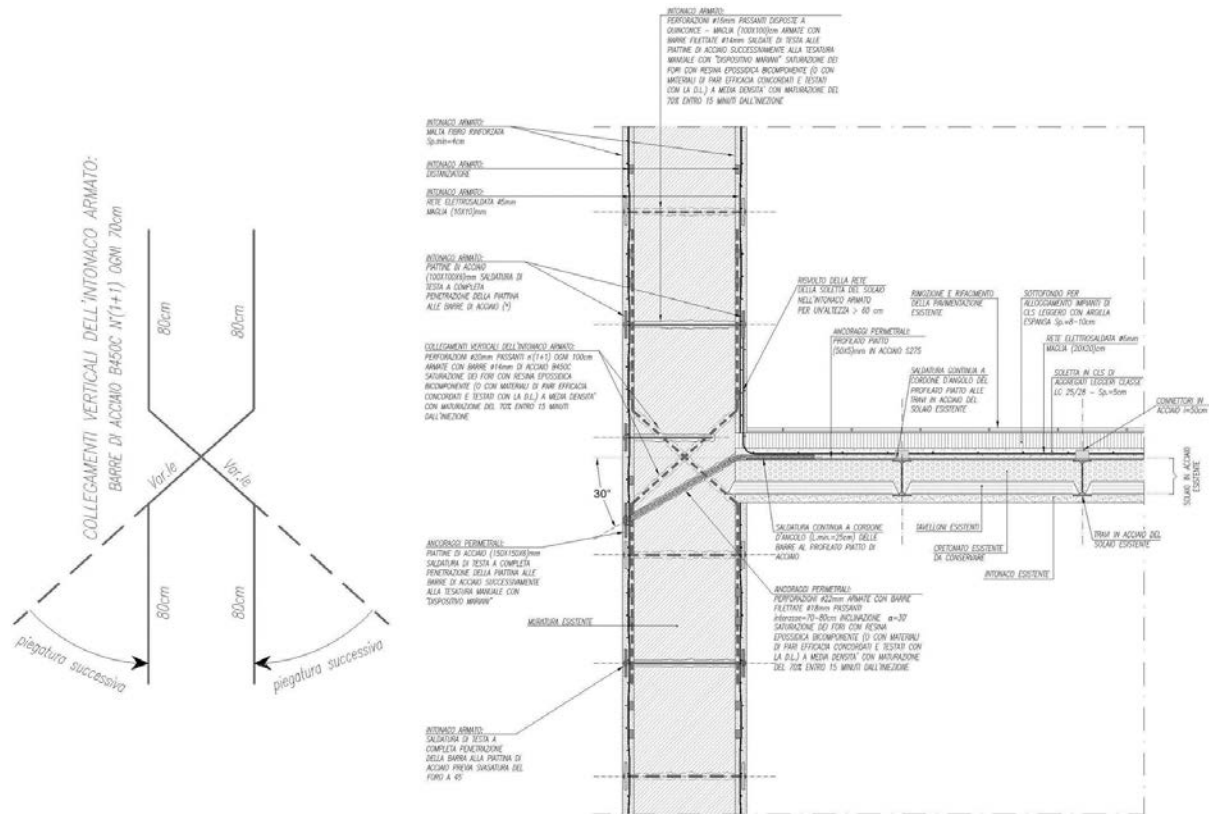


Figure 17. Floor-to-external-wall connection [1] in presence of reinforced mortar either traditional or innovative (e.g. CRM)

The masonry wall is supposed to be consolidated through traditional or innovative (e.g. CRM) reinforced plaster. The result is an increment of mechanical properties in terms of compressive and shear strength. This aspect is captured through flexure and diagonal cracking shear verifications of masonry panels under static and seismic actions. For example, in seismic analysis carried out with the pushover method, these safety verifications take into account strength and deformation capacity of masonry considering its elastic-plastic behavior.

In this kind of modelling, however, the structural joints, that is, the wall portions at the intersection between piers and spandrels or between piers and floors, are qualified as rigid zones and affect the structural response only because they reduce the effective length of masonry piers and spandrel.

In reality, as highlighted by recent studies [9], structural joints are affected by local phenomena which may play a crucial role for the equilibrium of the wall in terms of resistance and deformation, both in-plane and out-of-plane.

The study of jerk effects and impulsive nature of seismic action, suggests to pay particular attention towards floor-to-wall connections. As noted above, under impulsive actions, the areas characterized by structural discontinuity or by heterogeneity of materials (as in rubble stone masonry with poor quality mortar) are affected by stress concentration, thus it is necessary to assess the dynamic behavior of the involved local masses in order to counteract potential disaggregation. These effects are not addressed in the safety verifications normally applied in the context of seismic analysis.

To this end, Poisson's ratio ν is used to determine the transversal (horizontal) stress.

Figure 18 shows the local mass M involved by jerk impulsive action, consisting in the masonry mass M_m and the slab mass M_s . The longitudinal dimension b , along Y direction, can be determined considering both the spacing between load-bearing elements and the dimensions of the intersection between piers and spandrels. The thickness of the wall s and the height $4h$ (with h equal to the thickness s) provide the dimensions of the mass in transversal X and vertical Z direction respectively. As a working hypothesis, the slab portion corresponding to mass M_s is assigned the length $2h$.

The choice of these dimensions, in particular the height $4h$ of masonry mass and the width $2h$ of slab mass, come from the experience gained by the authors in the observation of crack patterns after significant seismic events. From a design point of view, the dimension h is linked both to the thickness of masonry and to the space required to place the transversal tensile elements.

Forces F_X and F_Z forces are the horizontal and vertical impulsive actions produced by jerk. The choice of direction is conventional; in this example F_X is oriented outwards and F_Z downwards.

The jerk actions relevant to the local mass M are defined by the relations linking impulsive force per unit mass to PGA , expressed, as already illustrated in the previous sections, by:

$$F_{imp,max,H} = 1.616 PGA_H \quad (7)$$

$$F_{imp,max,V} = 1.545 PGA_V \quad (8)$$

Based on typical dynamic characteristics of masonry buildings, the horizontal mean period of jerk is not very close to the horizontal natural periods of the building, while this is not the case for the vertical direction. This suggests that resonance phenomena may occur in the vertical direction.

Since the jerk mean frequency of the seismic event expected to strike the building is unknown, resonance condition is assumed for safety. Based on currently available data, in the definition of the impulsive forces we assume that jerk propagates through the building without modifications with respect to the ground.

This is reasonable for the vertical direction. For the horizontal direction, instead, Tong et al. [3] indicate that jerk undergoes at floor level an amplification similarly to what occur for acceleration; however, these indications still need to be verified in relation to various structural typologies. On these aspects, Research shall provide further results, identifying more precisely the propagation of jerk through buildings. As a matter of fact, studies on jerk response spectra are currently in progress [10].

According to the hypothesis, the impulsive forces in vertical direction are amplified by a factor $C_{ampl} = 5$. This amplification corresponds to resonance condition between structure and jerk assuming the equivalent viscous damping coefficient $\xi_{eq} = 10\%$, higher than what is normally considered (5%). In fact, we consider that masonry may already be cracked at the beginning of the seismic excitation, for example due to its non-cohesive nature or due to previous damages. During the expected seismic event, the development of progressive cracking would increase damping and reduce the amplifications due to resonance. However, the damages caused by impulsive actions are typically brittle and caused by instantaneous overcoming of resistance, and this can happen even at the beginning of the phenomenon. Moreover, it should

be considered that the highest vertical impulses frequently occur in the first phase of the event. For all these reasons, we assume that the equivalent viscous damping coefficient should not be higher than 10%.

Ultimately, the impulsive forces corresponding to mass M are calculated as follows:

$$F_X = 1.616 PGA_H \cdot M \quad (9)$$

$$F_Z = 1.545 PGA_V \cdot C_{ampl} \cdot M \quad (10)$$

Regarding the spatial simultaneity of jerk peaks, the available data (obtained processing records of the main seismic events in the Italian territory [1]) show that the phenomenon is continuously spatial and the jerk peaks in the three directions occur randomly. Precisely because of this randomness, it is not possible to exclude that significant peaks may occur simultaneously; therefore, in the safety verifications it is advisable to consider all three components of the impulsive actions. In this way under no circumstances the designed resistant elements would be insufficient.

With reference to Figure 18, the effects of F_Y force, orthogonal to the section plane, are distributed within the joint and absorbed by 4 longitudinal tensile elements placed in correspondence of the transversal reinforcements. These elements are necessary to achieve longitudinal continuity of the reinforcement also considering the shear effects generated by lateral expansion of masonry. In the section plane, forces F_Y and F_Z both contribute to the impulsive stresses.

Force F_Z generates the following vertical tension:

$$\sigma_Z = F_Z / bs \quad (11)$$

Being E the modulus of elasticity of masonry, vertical contraction ε_Z , transversal expansion ε_X and transversal tension σ_X are given by:

$$\varepsilon_Z = \sigma_Z / E, \quad \varepsilon_X = -\nu \varepsilon_Z = -\nu \sigma_Z / E, \quad \sigma_X = -\nu \sigma_Z \quad (12)$$

The transversal tensile elements must counteract the transversal tension σ_X acting on the lateral faces of the node, plus the transversal impulsive force F_X . Therefore, the tensile force that the elements must resist is given by:

$$T = \nu \sigma_Z \cdot 4h \cdot b + F_X \quad (13)$$

Regarding masonry Poisson's ratio, current Italian technical Standards consider $\nu = 0.5$ (calculated from E and G values given in NTC18, Tab. C8.5.I), thus this is the value used in the proposed formulation. A greater value would increase the transversal tension produced by the vertical force, but as far as observed it correspond to more cracked masonry which in turn is characterized by greater ξ_{eq} damping coefficient with consequent decrease of the resonance amplification factor; therefore, the two aspects compensate each other.

4.2 JERK-RESISTANT TRANSVERSAL AND BENT ELEMENTS

A second hypothesis of integrative elements aimed to counteract jerk effects consists in the use of bent tensile elements in addition to the transversal ones. In this case, the design can be carried out without considering the transversal behavior of masonry, thus disregarding the relation between vertical compressive and transversal tensile stress. This is achieved by considering that jerk impulsive forces are resisted by a truss-type structure where some elements resist tension and some other compression. Tensile stresses are used to design the additional transversal and bent elements, while the compressive stress acting on the struts must be compared with the compressive strength of masonry.

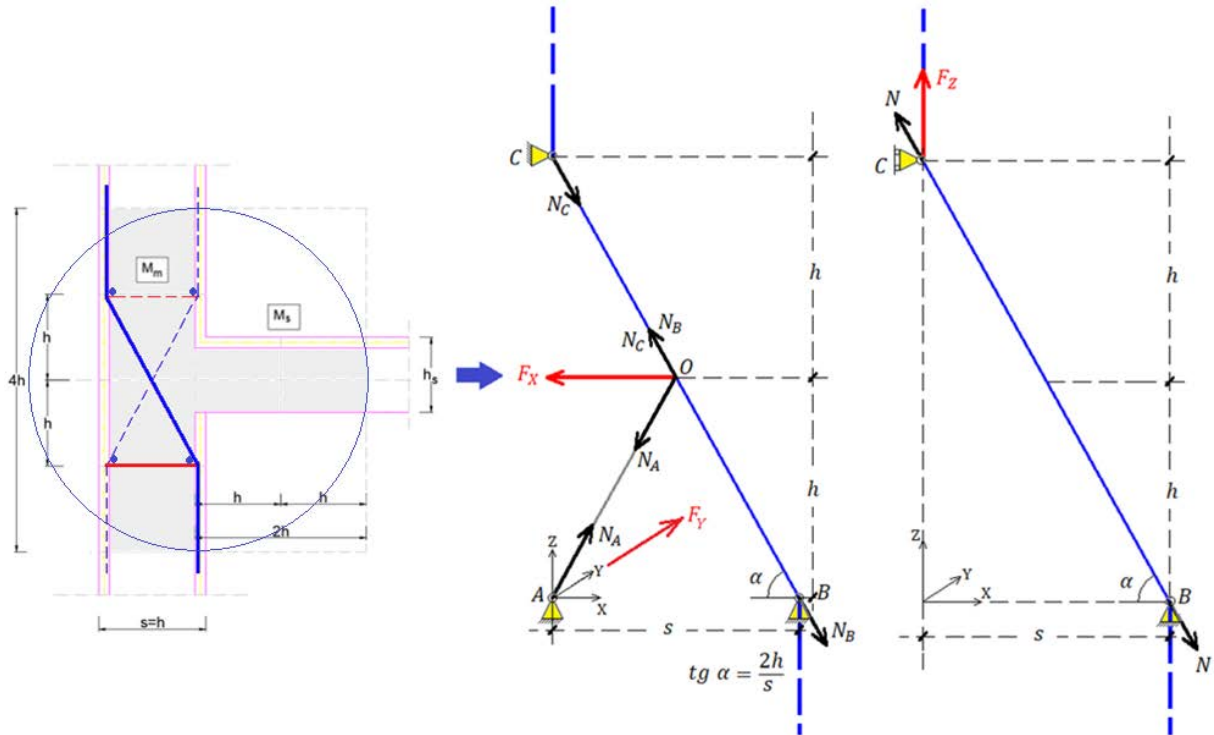


Figure 19. Additional truss-type elements to counteract impulsive actions.

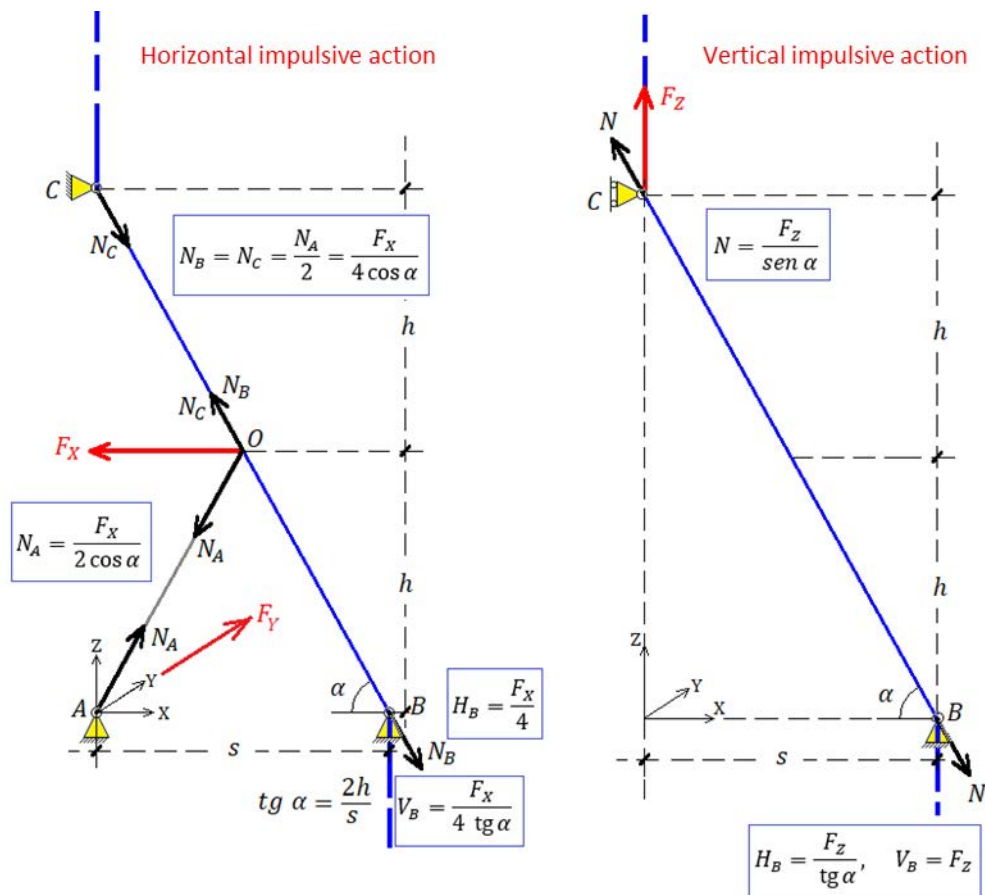


Figure 20. Internal actions in truss elements and joint reactions

Static scheme with horizontal impulsive action:

- axial forces:

$$N_A = \frac{F_X}{2 \cos \alpha}, \quad N_B = N_C = \frac{N_A}{2} = \frac{F_X}{4 \cos \alpha} \quad (14)$$

- joint reactions:

$$H_B = \frac{F_X}{4}, \quad V_B = \frac{F_X}{4 \tan \alpha} \quad (15)$$

Static scheme with horizontal impulsive action:

- axial forces:

$$N = \frac{F_Z}{\sin \alpha} \quad (16)$$

- joint reactions:

$$H_B = \frac{F_Z}{\tan \alpha}, \quad V_B = F_Z \quad (17)$$

Ultimately, bent element verification is applied considering the following tensile force:

$$N_{bent} = \frac{F_X}{4 \cos \alpha} + \frac{F_Z}{\sin \alpha} \quad (18)$$

While for the tensile verification of the transversal elements:

$$N_{trans} = \frac{F_X}{4} + \frac{F_Z}{\tan \alpha} \quad (19)$$

Proper anchorage of the bent elements is ensured selecting an adequate length of the vertical segments.

The additional compressive stress due to jerk is considered applied in the compressed strut having section A_p . Assuming σ_v as the vertical compressive stress in the wall due to the acting loads (static and seismic), and f_d as the design compressive strength of masonry, the maximum bearable compressive stress due to jerk impulsive action is given by:

$$\sigma_{j,max} = f_d - \sigma_v \quad (20)$$

This must be compared with the actual stress caused by jerk, which considering the inclination of the strut is expressed by:

$$\sigma_j = (N_A/A_p) \cdot \sin \alpha = \frac{F_X \tan \alpha}{2 \cdot A_p} \quad (21)$$

4.3 APPLICATION EXAMPLE

The following example refers to a masonry building located near Perugia (Italy). The design seismic action at the Ultimate Limit State of Significant Damage is characterized by: (i) in horizontal direction $a_g = 0.186g$ and $S = 1.2$, thus $PGA_H = 0.223g$; (ii) in vertical direction $a_{gV} = 0.186g$ and $S = 1.0$, thus $PGA_V = 0.186g$.

The building consists of two stories (ground floor and first floor) and its load bearing walls are made of rubble stone masonry with specific weight $w = 19 \text{ kN/m}^3$. The fundamental period of vibration in horizontal direction is equal to 0.378 sec , while in vertical direction it is equal to 0.058 sec .

Considering the representative mean periods of acceleration and jerk given in Table 2, it can be observed that the jerk mean period in horizontal direction (about 0.100 sec) is far from the fundamental period of the building (0.378 sec); while in the vertical direction the two periods

are very close (*0.078 sec for jerk, 0.058 sec for the building*). Therefore, as noted above, resonance phenomena may occur in vertical direction.

Let us consider a floor-to-wall connection with the following dimensions (see Figure 18): $s = 400$ mm, $h = s = 400$ m, $b = 1000$ mm. The masonry mass involved in the local impulsive phenomena corresponds to the following weight:

$$P_m = wsb \cdot 4h = 19.00 \cdot 0.40 \cdot 1.00 \cdot 4 \cdot 0.40 = 12.16 \text{ kN} \quad (22)$$

The floor is characterized by 2.50 kN/m^2 permanent load and 2.00 kN/m^2 vertical load with seismic combination coefficient $\psi_2 = 0.3$; therefore, the slab mass M_s corresponds to distributed load of 3.1 kN/m^2 and its total weight is given by:

$$P_s = (g + \psi_2 q) \cdot 2h \cdot b = 3.10 \cdot 0.8 \cdot 1.00 = 2.48 \text{ kN} \quad (23)$$

The total node weight and the corresponding impulsive forces are the following:

$$P = 12.16 + 2.48 = 14.64 \text{ kN} \quad (24)$$

$$F_x = 1.616 \cdot 0.223 \cdot 14.64 = 5.28 \text{ kN} \quad (25)$$

$$F_z = 1.545 \cdot 0.186 \cdot 5 \cdot 14.64 = 21.03 \text{ kN} \quad (26)$$

STRENGTHENING THROUGH TRANSVERSAL ELEMENTS

The transversal tensile force resisted by the additional transversal elements (cf. section 3.1) is given by the following expressions:

$$\sigma_z = 21030 / (1000 \cdot 400) = 0.053 \text{ N/mm}^2 \quad (27)$$

$$T = 0.5 \cdot 0.053 \cdot 1600 \cdot 1000 + 5280 = 47680 \text{ N} \quad (28)$$

Considering the insertion of 2 steel bars type B450C $\phi 12$ (section 113 mm^2) at the intrados and extrados of the floor with longitudinal spacing of 1.00 m, the total resistant cross section is 226 mm^2 .

Considering a partial safety factor $\gamma_s = 1.15$, the design yield strength is given by $450/1.15 = 391 \text{ N/mm}^2$. Moreover, considering a confidence factor $CF = 1.20$ corresponding to knowledge level KL2, the safety verification is given by:

$$\sigma_s = \frac{47680}{226} = 211 < \frac{391}{1.20} = 325 \frac{\text{N}}{\text{mm}^2} \quad (29)$$

Expression (29) yields a safety factor equal to 1.54 . This value can be considered satisfactory considering the actual ground acceleration registered in previous seismic events. Therefore, robustness is ensured even with respect of peak ground acceleration and jerk higher than those considered as design values.

For the longitudinal Y direction, we consider the insertion of 4 longitudinal bars $\phi 10$ (total cross section 314 mm^2) in correspondence of the ends of the transversal elements. Therefore:

$$F_Y = F_X = 5.28 \text{ kN} \Rightarrow \sigma_s = \frac{5280}{314} = 17 \frac{\text{N}}{\text{mm}^2} \quad (30)$$

$$F = \sqrt{F_X^2 + F_Z^2} = \sqrt{21.03^2 + 5.28^2} \text{ kN} = 21.68 \text{ kN} \Rightarrow \tau_s = \frac{21680}{314} = 69 \frac{\text{N}}{\text{mm}^2} \quad (31)$$

$$\sigma_s^2 + 3 \tau_s^2 = 17^2 + 3 \cdot 69^2 = 14572 < 325^2 = 105625 \quad (32)$$

Although the proposed elements turn out to be oversized, their contribution, as already noted, is necessary to achieve longitudinal continuity of the reinforcement also considering the shear effects generated by lateral expansion of masonry.

The influence of masonry typology on the impulsive action effects can be evaluated by considering the behavior of the structural node without consolidation. In this example, the additional transversal elements have been entrusted with a total tensile force $T = 47680$ N. In the absence of reinforcements, masonry would increase the possibility to develop cracks perpendicular to the tensile stress, that is, in the hypothesis of centered axial force, vertical cracks. The tensile strength can be assumed, as a first approximation, equal to the shear strength ($f_{td} \cong \tau_{od}$); therefore, the acting stress is given by:

$$\tau = T/(b \cdot 4h) = 47680/(1000 \cdot 1600) = 0.030 \text{ N/mm}^2 \quad (33)$$

According to strength values suggested by Italian technical standard with respect to knowledge level KL2 ($CF = 1.2$), rubble stone masonry is characterized by $\tau_{od} = 0.025 / 1.2 = 0.021 \text{ N/mm}^2$. Therefore, under the hypothesis of this example, masonry alone without reinforcement would not satisfy the safety verification.

Considering nodes with the same geometry as the one in the example, it is interesting to determine for various masonry typologies the limit value of PGA beyond which the jerk effects, in the case of maximum amplification, would generate local damages.

Table 4 reports those limit values for various masonry typologies. The results were obtained, based on what illustrated above, by applying expression (13) and considering knowledge level KL2:

$$T = v \frac{F_z}{b_s} \cdot 4h \cdot b + F_x = 0.5 \frac{(1.545 PGA_V \cdot 5 \cdot P)}{b_s} \cdot 4h \cdot b + 1.616 PGA_H \cdot P \quad (34)$$

$$P = w s b \cdot 4h + (g + \psi_2 q) \cdot 2h \cdot b$$

The limit value of ground acceleration a_g was obtained considering:

$$PGA_V = a_{gV} = a_g, \quad PGA_H = 1.2 \cdot a_g, \quad T = b \cdot 4h \cdot \tau_{od}$$

| Masonry typology | τ_{od} (N/mm ²) | w (kN/m ³) | a_g (g) |
|--|----------------------------------|--------------------------|-----------|
| Rubble stone | 0.021 | 19 | 0.132 |
| Roughly hewn stone | 0.036 | 20 | 0.217 |
| Split stone | 0.054 | 21 | 0.312 |
| Irregular soft stone (tuff, calcarenite, etc.) | 0.029 | 16 | 0.209 |
| Regular soft stone (tuff, calcarenite, etc.) | 0.050 | 16 | 0.362 |
| Ashlar stone | 0.0875 | 22 | 0.486 |
| Solid bricks and lime mortar | 0.075 | 18 | 0.493 |
| Semi solid bricks and cement mortar | 0.104 | 15 | 0.792 |

Table 4. Limit ground acceleration with respect to various masonry typologies

As shown in Table 4, masonry typologies of better quality can withstand impulsive actions corresponding to higher ground accelerations. In case of rubble stone masonry local damage in the structural node can occur for ground acceleration higher than 0.132 g. Instead, in case of ashlar masonry or brick masonry this type of failure is unlikely to occur since very high ground accelerations would be required (around 0.490 g).

Rubble, roughly hewn or split stone are the masonry typologies that require particular attention as far as regard the strengthening of structural nodes. After all, these are also the masonry typologies that most frequently need interventions, such as grout injections and/or reinforced plaster. Therefore, the additional strengthening elements proposed in the present work would be mainly applied to these types of masonry.

STRENGTHENING THROUGH TRANSVERSAL AND BENT ELEMENTS

For the intervention with bent elements along with transversal elements we refer to the formulation given in section 3.2. On top of the data already given for the example, let us consider: $\alpha = 63.43^\circ$, $\sin \alpha = 0.894$, $\cos \alpha = 0.447$, $\tan \alpha = 2$ (Figure 19).

The tensile force verification in the bent bar is expressed by:

$$A_{min} = \frac{\frac{F_X}{4 \cos \alpha} + \frac{F_Z}{\sin \alpha}}{f_{yd}} = \frac{\frac{5280}{4 \cdot 0.447} + \frac{21030}{0.894}}{391} = \frac{2953 + 23523}{391} = \frac{26476}{391} = 68 \text{ mm}^2 \quad (35)$$

Let us consider the placement of $\phi 14$ bent rebars (section 154 mm^2) with spacing between elements with same bending direction equal to 1400 mm . The effective section must be corrected by the factor $1000/1400=0.7$. Ultimately the tensile stress due to impulsive actions is given by:

$$\sigma = \frac{26476}{154 \cdot 0.7} = 246 \text{ N/mm}^2 \quad (36)$$

Thus, the safety verification is satisfied with a safety factor equal to $391/246 = 1.59$.

Consider insertion of $\phi 14$ transversal rebars placed according to a quincunx layout with spacing equal to 1000 mm . The tensile stress they should resist is given by:

$$N = \frac{F_X}{4} + \frac{F_Z}{\tan \alpha} = \frac{5280}{4} + \frac{21030}{2} = 11835 \text{ N} \quad (37)$$

$$\sigma = \frac{11835}{(1000 \cdot 1600)/(1000 \cdot 1000) \cdot 154} = 48 \text{ N/mm}^2 \quad (38)$$

Therefore, the transversal tensile elements are subjected to a significant lower stress compared to the case without bent elements (211 N/mm^2).

A remark about the different structural behavior achieved through the two proposed interventions is required. The transversal elements by themselves can counteract the jerk impulsive actions. However, the bent elements may ensure structural continuity of reinforced plaster in correspondence of the floor-to-wall connection, an aspect which is generally neglected, particularly in the connection between floors and load-bearing internal walls. The discontinuity of the reinforced plaster at the intrados and extrados of floors may in fact be the cause of local vulnerability.

Ultimately, as far as regards the compression verification of masonry strengthened through reinforced plaster, the compressive strength is evaluated according to technical Standards (NTC2018) applying an amplification factor equal to 2.5: $f_m = 2.5 \cdot 1.5 = 3.75 \text{ N/mm}^2$, then, considering a confidence factor $CF = 1.2$, $f_d = 3.75/1.2 = 3.125 \text{ N/mm}^2$.

In the case under examination, the local mass affected by local impulsive actions is assumed to have a depth of 1000 mm . However, conservatively we consider that the strut will form in correspondence of the truss. Its cross section is assumed to be equal to $b \cdot \mu s$, with coefficient of thickness reduction μ that can be assumed equal to 0.2. Therefore, the strut cross section is equal to $A_p = 1000 \cdot 0.2 \cdot 400 = 80000 \text{ mm}^2$. Thus, the compressive stress in the strut is given by:

$$\sigma_j = \frac{\frac{F_X}{2 \cos \alpha}}{A_p} = \frac{\frac{5280}{2 \cdot 0.447}}{80000} = 0.07 \text{ N/mm}^2 \quad (39)$$

It corresponds to a small fraction of masonry compressive strength ($0.07 / 3.125 = 2\%$); therefore, it is reasonable to assume that masonry can act as strut in the truss-type behavior. This proves that, under the effects of impulsive forces, masonry itself, strengthened with

reinforced plaster, can resist the additional compressive stress. Instead, the proposed strengthening elements counteract the jerk effects by providing additional tensile strength.

5 CONCLUSIONS

In existing masonry buildings, the design of strengthening interventions, both in case of repair or prevention, must ensure the proper connection of the floors to the load-bearing walls. However, this may not be sufficient to avoid local damages under jerk impulsive effects, with potential loss of robustness and trigger of progressive chaotic collapses, particularly fearsome in case of rubble stone masonry with poor quality mortar.

Therefore, the equilibrium and the resistance of floor-to-wall connections must also be assessed in relation to the continuous acceleration variation, which can generate local impulsive actions significantly higher than static and seismic inertial actions, with consequent stress concentrations and potential masonry disaggregation.

Confinement of masonry and insertion of tensile resistant elements aimed to absorb the impulsive stresses are necessary. Additional transversal tensile elements represent a natural extension of the reinforced plaster intervention, both in case of traditional and innovative techniques.

With the addition of bent tensile elements the continuity of the reinforced plaster in correspondence of structural nodes can be ensured, an aspect which is generally neglected, particularly in the connection between floor and load-bearing internal walls. The discontinuity of the reinforced plaster at the intrados and extrados of floors may in fact be the cause of local vulnerability.

ACKNOWLEDGEMENTS

The authors appreciate the support of colleagues and collaborators that contributed to this research. They would like to thank Luca Ranocchia, Alessia Travanti and Nicola Pero Nullo for the composition and drawing of the construction details; Fulvio Massimo Mariani for the selection of records on ITACA database; Alessio Francioso for the elaborations of Fourier spectra and his support in the revision of this article. They also wish to thank Aedes Software for the software Seismic3D developed by Francesco Pugi as part of applied research activities.

REFERENCES

- [1] M. Mariani, F. Pugi, Jerk: effetti delle azioni sismiche impulsive e crisi locali nelle strutture in muratura, *Ingenio*, 2020
- [2] M. Mariani, F. Pugi, Effects of Impulsive Actions Due to Seismic Jerk and Local Failures in Masonry Structures, *Eurodyn 2020*, Athens, Greece, 23–26 November 2020
- [3] M. Tong, G.Q. Wang, G.C. Lee, Time derivative of earthquake acceleration, *Earthquake Engineering and Engineering Vibration*, Vol. 4, No. 1, 1-16, June, 2005.
- [4] M. Mariani, F. Pugi, A. Francioso, Sisma verticale: modellazione e analisi in ambito professionale sugli edifici esistenti in muratura, *Ingenio*, 01.10.2018
- [5] N. Chieffo, A. Formisano, P. Lourenco: Seismic vulnerability procedures for historical masonry structural aggregates: Analysis of the historical centre of Castelpoto (South Italy), *Structures* 48 (2023), 852-866.

- [6] E.M. Rathje, N.A. Abrahamson, J.D. Bray, Simplified frequency content estimates of earthquake ground motions, *J. Geotech. Geoenviron. Eng.*, 124(2), 150-159, 1998.
- [7] V. Vukobratovic: The influence of jerk on the seismic responses of rigid linear elastic and nonlinear sdof systems, April 2022. Conference: 19th International Symposium of MASEAt: Ohrid, North Macedonia.
- [8] V. Vukobratovic, S. Ruggieri: Jerk in Earthquake Engineering: State-of-the-Art, *Buildings* 2022, 12, 1123.
- [9] C. Sansoni, Luís C.M. da Silva, R. Marques, S. Pampanin, Paulo B. Lourenço: SLaMA-URM method for the seismic vulnerability assessment of UnReinforced Masonry structures: Formulation and validation for a substructure, *Journal of Building Engineering*, Volume 63, Part A, 2023, 105487, ISSN 2352-7102,
- [10] Haoxiang He, Ruifeng Li, Kui Chen: Characteristics of Jerk Response Spectra for Elastic and Inelastic Systems, *Shock and Vibration*, Vol. 2015, Article ID 782748.